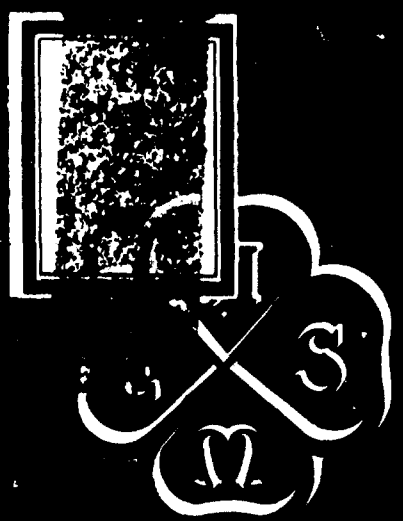

AN
ASME
PUBLICATION

50¢ PER COPY
40¢ TO ASME MEMBERS

THE AMERICAN SOCIETY OF MECHANICAL ENGINEERS
29 West 39th Street, New York 18, N. Y.

1960
PAPER NUMBER 59-IRD-6

Dynamic Response and Control of Multipass Heat Exchangers

MASAMI MASUBUCHI

Assistant Professor, Faculty of Engineering, Yokohama National University, Yokahama, Japan.

The transfer functions obtained by dynamic analysis of one shell pass and 2, 3, 4, ——, 2n, 2n+1 tube-pass heat exchangers as a distributed parameter system are presented in dimensionless forms. The heat-exchange processes are found to be governed by the third-order characteristic equations with complex coefficients, and can be solved numerically using a graphical method. The numerical examples are presented to show the clear difference of frequency response for such cases when no solid capacity exists. The analog computer and the experimental results are found to be in good agreement with the theoretical results.

For presentation at the Instruments and Regulators Conference, Cleveland, Ohio, March 29—April 2, 1959, of The American Society of Mechanical Engineers. Manuscript received at ASME Headquarters, September 22, 1958.

Written discussion on this paper will be accepted up to May 4, 1959.

Copies will be available until January 1, 1960.

Dynamic Response and Control of Multipass Heat Exchangers

MASAMI MASUBUCHI

Introduction

Pure parallel-and counterflow heat exchangers have been analyzed exactly [1],[2] and their controllability have been extensively discussed in the literatures [3,4,5]. For multi-pass heat exchangers, many kinds of researches on the mean temperature difference [6 ~ 10] and on steady temperature distributions [11] have been published, but there have been few on dynamic analysis.

However, from the control engineer's point of view, process dynamics is one of the most important subjects.

The dynamic response of the system is dependent not only on the mean temperature difference, but also on other system parameters such as fluid velocities, heat capacities of the fluids and tube-walls, etc.. The transient response seems quite difficult to calculate, but the frequency response analysis is simpler and is used throughout this paper.

The author extended the P.Profos's basic partial differential equation [12] and analyzed exactly the dynamic characteristics of 1-2,3,4, --- ,2n,2n+1 pass heat exchangers.

The 3rd order characteristic equations governing the heat exchange processes in each multi-pass heat exchanger, and the transfer function formulas which involve the roots of the said equation are obtained and presented.

Numerical examples of frequency response of each case with no solid capacity have also been shown.

Nomenclature

The following nomenclature is used in this paper:

A	m^2	= heat exchange surface area
a	dl.	= kA/q, $a_1 = kA/q_1$

---

[1] Numbers in parentheses refer to similarly numbered references in bibliography at the end of the paper.

a'	dl.	$= hA/q$, $a_1' = h_1A/q_1$, $a_s' = h_sA/q$
b	dl.	$= hA/(Cv)$, $b_1 = hA/(C_hv_1)$, $b_2 = h_1A/(C_hv_1)$, $b_s = h_sA/(C_sv_1)$
C	kcal/m°C	= series and side capacity
H	m	= total length of shell
h	kcal/m²mn°C	= film coefficient of heat transfer, h_1 tube-side, h shell-side, h_s side capacity-side
k	kcal/m²mn°C	= overall coefficient of heat transfer
L	mn	= dead time, $H/v = L$, $H/v_1 = L_1$
l	dl.	$= Y/H$
p		= variable in auxiliary equation
q	kcal/mn°C	$= vw$, $q_1 = v_1w_1$
r	dl.	$= v_1/v = L/L_1$
s	dl.	$= j\omega$, $j = \sqrt{-1}$
t	mn	= time
U	m	= peripheral length of heat exchange surface
u		= variable (see Appendix)
v		= variable (see Appendix)
or	m/mn	= fluid velocity, v_1 tube-side, v shell-side
w	kcal/m°C	= heat capacity of fluid per unit length
Y	m	= running length of shell measured from shell input
$\alpha_1, \alpha_2, \alpha_3$		= parameters defined by Equation (3)
$\beta_1, \beta_2, \beta_3$		= parameters defined by Equation (3)
Ⓗ	°C	= temperature of shell fluid in lumped system
θ	°C	= temperature of fluid, θ shell-side, $\theta_1, \theta_2, \theta_3$, --- tube-side
τ	dl.	$= t/L_1$
φ	°C	= temperature of solid, φ_h series capacity, φ_s side capacity
ω	dl.	= circular frequency
and	dl.	= dimensionless

Subscripts: 1,2,3, -- = tube-side, no subscript = shell-side
i = input, o = output
h = series capacity, s = side capacity

Basic Assumptions

1. Fluid velocities, heat transfer coefficients are all constant and do not change with the temperature of fluid or heat exchange surfaces.
2. Each cross section is constant.
3. Complete mixing in crosswise directions of each flow exists.

4. The heat conductivi of tube-and shell-walls are infinite in the directions at ri angles to the flow and zero in flow directions.
5. There is no heat loss to outer circumferences.

The transfer function is taken to be the dynamic ratio of the outlet temperature of one fluid to the inlet temperature of another fluid. Considering sinusoidal solution, sinusoidal temperature variation is superposed on the steady state temperature, so the above definition is enough to consider.

Fundamental Equations

The following relation exists between a fluid at temperature θ and a solid surface at temperature φ through which heat exchange takes place.

$$\frac{\partial\theta}{\partial t}+\frac{\partial\theta}{\partial Y}\cdot v=\frac{hU}{w}(\varphi-\theta)$$

Using nondimensional τ, ℓ and a', gives

$$\frac{\partial\theta}{\partial\tau}+\frac{\partial\theta}{\partial\ell}=a'(\varphi-\theta)$$

If the tube-wall is infinitely thin, φ can be replaced by the temperature of another fluid, and a' replaced by a. This fundamental equation applies to θ,θ_1,θ_2, --- in the following.

1-2 Pass Heat Exchanger (13)

Case P-C:

The "P-C" flow pattern is shown in Fig.1. In this case, the tube fluid flows first from left to right, turns around at the right end, and finally flows back to the left, resulting in a parallel-flow followed by a counter flow. The shell fluid is always assumed to flow from the left end to the right end. Both inside and outside tube-walls are assumed to be infinitely thin so that there will be neither series nor side capacity to be considered.

Assuming equal dimensions and conditions for each tube-pass and

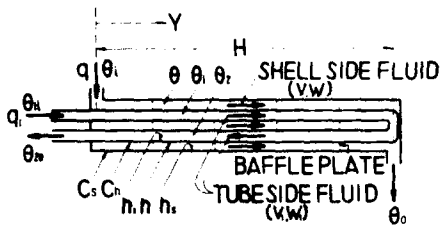

Fig.1 1-2 pass heat exchanger snowing symbolism.

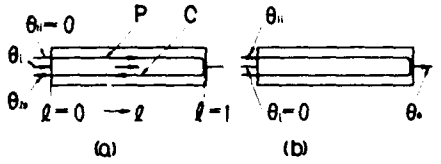

Fig.2 Case P-C (a) shell-side input; (b) tube-side input.

equal U for shell-and tube-fluid, the fundamental equations are,

$$\begin{cases} \frac{\partial\theta_1}{\partial\tau} + \frac{\partial\theta_1}{\partial l} = a_1(\theta - \theta_1) \\ \frac{\partial\theta_2}{\partial\tau} - \frac{\partial\theta_2}{\partial l} = a_1(\theta - \theta_2) \\ r\frac{\partial\theta}{\partial\tau} + \frac{\partial\theta}{\partial l} = a(\theta_1 + \theta) + a(\theta_2 - \theta) \end{cases} \tag{1}$$

The solution of Equations (1) for a sinusoidal input signal ($e^{s\tau}$) are

$$\begin{cases} \theta_1 = (\beta_1 C_1 e^{p_1 l} + \beta_2 C_2 e^{p_2 l} + \beta_3 C_3 e^{p_3 l})\, e^{s\tau} \\ \theta_2 = (\alpha_1 C_1 e^{p_1 l} + \alpha_2 C_2 e^{p_2 l} + \alpha_3 C_3 e^{p_3 l})\, e^{s\tau} \\ \theta = (C_1 e^{p_1 l} + C_2 e^{p_2 l} + C_3 e^{p_3 l})\, e^{s\tau} \end{cases} \tag{2}$$

where, C_1, C_2, C_3 are the integration constants, and α, β are:

$$\begin{cases} \alpha_1 = \frac{a_1}{-p_1 + s + a_1}, \quad \alpha_2 = \frac{a_1}{-p_2 + s + a_1}, \quad \alpha_3 = \frac{a_1}{-p_3 + s + a_1} \\ \beta_1 = \frac{a_1}{p_1 + s + a_1}, \quad \beta_2 = \frac{a_1}{p_2 + s + a_1}, \quad \beta_3 = \frac{a_1}{p_3 + s + a_1} \end{cases} \tag{3}$$

p_1, p_2, p_3 are the three roots of

$$p^3 + p^2(2a + rs) - p(s + a_1)^2 - s(s + a_1)\{r(s + a_1) + 2a\} = 0 \tag{4}$$

The roots are all complex (see Appendix).

Shell-side input: The C_1, C_2, C_3 can be determined from the following boundary conditions (Fig.2(a)).

$$l = 0: \quad \theta_1 = \theta_{1i} = \beta_1 C_1 + \beta_2 C_2 + \beta_3 C_3 = 0$$

$$l = 1: \quad \theta_1 = \theta_2, \text{ or } \beta_1 C_1 e^{p_1} + \beta_2 C_2 e^{p_2} + \beta_3 C_3 e^{p_3} = \alpha_1 C_1 e^{p_1} + \alpha_2 C_2 e^{p_2} + \alpha_3 C_3 e^{p_3}$$

The substitution of the results thus obtained into Equations (2)

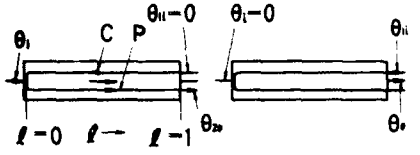

Fig.3 Case C-P (a) shell-side input; (b) tube-side input.

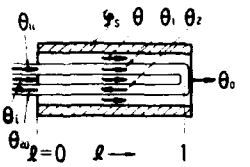

Fig.4 With side capacity.

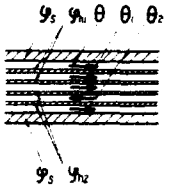

Fig.5 With series and side capacity.

and solving for θ_{20}/θ_i (= $G_{PC-st}(s)$) gives the transfer function.

$$G_{pc-st}(s) = \frac{(\alpha_1-\beta_1)(\alpha_2\beta_3-\alpha_3\beta_2)e^{p_1} + (\alpha_2-\beta_2)(\alpha_3\beta_1-\alpha_1\beta_3)e^{p_2} + (\alpha_3-\beta_3)(\alpha_1\beta_2-\alpha_2\beta_1)e^{p_3}}{(\alpha_1-\beta_1)(\beta_3-\beta_2)e^{p_1} + (\alpha_2-\beta_2)(\beta_1-\beta_3)e^{p_2} + (\alpha_3-\beta_3)(\beta_2-\beta_1)e^{p_3}} \tag{5}$$

If input and output are exchanged with each other (Fig.2(b)), we obtain the following transfer function through a similar procedure:

$$G_{pc-ts}(s) = \frac{[\alpha_2-\beta_2-(\alpha_1-\beta_1)]e^{p_1+p_2} + [\alpha_3-\beta_3-(\alpha_2-\beta_2)]e^{p_2+p_3} + [\alpha_1-\beta_1-(\alpha_3-\beta_3)]e^{p_3+p_1}}{(\alpha_1-\beta_1)(\beta_3-\beta_2)e^{p_1} + (\alpha_2-\beta_2)(\beta_1-\beta_3)e^{p_2} + (\alpha_3-\beta_3)(\beta_2-\beta_1)e^{p_3}} \tag{6}$$

Static Characteristics:

This is the case when s=0 in Equations (5),(6). For s=0, from Equation (4), three roots are

$$p_1 = 0, \quad p_{2,3} = -a \pm \sqrt{a^2 + a_1^2}$$

which give

$$\begin{cases} \alpha_1 = 1, & \alpha_2 = \dfrac{a_1}{a_1 - p_2}, & \alpha_3 = \dfrac{a_1}{a_1 - p_3} \\ \beta_1 = 1, & \beta_2 = \dfrac{a_1}{a_1 + p_2}, & \beta_3 = \dfrac{a_1}{a_1 + p_3} \end{cases}$$

Introducing these values into Equations (5),(6), and rearranging, we obtain

$$G_{pc-st}(0) = \frac{2a_1}{a_1 + a + \sqrt{J}\coth\sqrt{J}} \tag{5'}$$

and

$$G_{pc-ts}(0) = \frac{2a}{a_1 + a + \sqrt{J}\coth\sqrt{J}} \tag{6'}$$

where, $J = a^2 + a_1^2$

(5'),(6') are the static characteristics known as temperature efficiency of the heat exchanger [14].

Case C-P:

Counterflow at input side, parallel-flow at output side (See Fig.3). The fundamental equations are as follows,

$$\begin{cases} \dfrac{\partial\theta_1}{\partial\tau} - \dfrac{\partial\theta_1}{\partial\ell} = a_1(\theta - \theta_1) \\ \dfrac{\partial\theta_2}{\partial\tau} + \dfrac{\partial\theta_2}{\partial\ell} = a_1(\theta - \theta_2) \\ r\dfrac{\partial\theta}{\partial\tau} + \dfrac{\partial\theta}{\partial\ell} = a(\theta_1 - \theta) + a(\theta_2 - \theta) \end{cases} \tag{7}$$

By solving these equations, the 3rd order characteristic equation identical to Equation (4) can be obtained. The temperatures are:

$$\begin{cases} \theta_1 = (\alpha_1 C_1 e^{k_1\ell} + \alpha_2 C_2 e^{k_2\ell} + \alpha_3 C_3 e^{k_3\ell})\, e^{s\tau} \\ \theta_2 = (\beta_1 C_1 e^{k_1\ell} + \beta_2 C_2 e^{k_2\ell} + \beta_3 C_3 e^{k_3\ell}) e^{s\tau} \\ \theta = (C_1 e^{k_1\ell} + C_2 e^{k_2\ell} + C_3 e^{k_3\ell}) e^{s\tau} \end{cases} \tag{8}$$

where, C_1, C_2, C_3 are the constants of integration, α, β can be expressed by the same equation as (3). Through the same procedure as before, we get

$$G_{cp\text{-}st}(s) = \frac{(\beta_2\alpha_3 - \alpha_2\beta_3)(\beta_1 - \alpha_1)e^{k_1+k_2} + (\alpha_3\beta_2 - \alpha_2\beta_3)(\beta_1 - \alpha_1)e^{k_2+k_3} + (\alpha_1\beta_3 - \alpha_3\beta_1)(\beta_2 - \alpha_2)e^{k_3+k_1}}{\alpha_1[\beta_2 - \alpha_2 - (\beta_3 - \alpha_3)]e^{k_1} + \alpha_2[\beta_3 - \alpha_3 - (\beta_1 - \alpha_1)]e^{k_2} + \alpha_3[\beta_1 - \alpha_1 - (\beta_2 - \alpha_2)]e^{k_3}} \tag{9}$$

$$G_{cp\text{-}ts}(s) = \frac{[\beta_2 - \alpha_2 - (\beta_3 - \alpha_3)]e^{k_1} + [\beta_3 - \alpha_3 - (\beta_1 - \alpha_1)]e^{k_2} + [\beta_1 - \alpha_1 - (\beta_2 - \alpha_2)]e^{k_3}}{\alpha_1[\beta_2 - \alpha_2 - (\beta_3 - \alpha_3)]e^{k_1} + \alpha_2[\beta_3 - \alpha_3 - (\beta_1 - \alpha_1)]e^{k_2} + \alpha_3[\beta_1 - \alpha_1 - (\beta_2 - \alpha_2)]e^{k_3}} \tag{10}$$

The static characteristics are,

from Equation (9) $\quad G_{cp\text{-}st}(0) = \dfrac{2a_1}{a_1 + a + \sqrt{J}\coth\sqrt{J}}$

from Equation (10) $\quad G_{cp\text{-}ts}(0) = \dfrac{2a}{a_1 + a + \sqrt{J}\coth\sqrt{J}}$

With Side Capacity

Assume that the side capacity (thermal capacity of shell wall) has infinite thermal resistance in the axial and no thermal resistance in the radial directions.

In the case P-C (same as C-P), for example, the fundamental equations are (See Fig.4)

$$\begin{cases} \frac{\partial\theta_1}{\partial\tau} + \frac{\partial\theta_1}{\partial l} = a_1(\theta-\theta_1) \\ \frac{\partial\theta_2}{\partial\tau} - \frac{\partial\theta_2}{\partial l} = a_1(\theta-\theta_2) \\ r\frac{\partial\theta}{\partial\tau} + \frac{\partial\theta}{\partial l} = a(\theta_1-\theta)+a(\theta_2-\theta)+a_s'(\varphi_s-\theta) \\ \frac{\partial\varphi_s}{\partial\tau} = b_s(\theta-\varphi_s) \end{cases} \tag{11}$$

In this case, the characteristic equation (4) changes somewhat and takes the following form

$$p^3 + p^2\left(2a + rs + \frac{a_s's}{s+b_s}\right) - p(s+a_1)^2 - s(s+a_1)\left\{r(s+a_1)+2a+\frac{a_s'}{s+b_s}(s+a_1)\right\} = 0 \tag{12}$$

With Series and Side Capacity

Assume that the series (solid capacity of tube-wall) and side capacity have infinite thermal resistance in the axial and no resistance in the radial directions. In the case of P-C, for example, the fundamental equations are (See Fig.5),

$$\begin{cases} \frac{\partial\theta_1}{\partial\tau} + \frac{\partial\theta_1}{\partial l} = a_1'(\varphi_{h1}-\theta_1) \\ \frac{\partial\theta_2}{\partial\tau} - \frac{\partial\theta_2}{\partial l} = a_1'(\varphi_{h2}-\theta_2) \\ r\frac{\partial\theta}{\partial\tau} + \frac{\partial\theta}{\partial l} = a'(\varphi_{h1}-\theta)+a'(\varphi_{h2}-\theta)+a_s'(\varphi_s-\theta) \\ \frac{\partial\varphi_{h1}}{\partial\tau} = b_1(\theta-\varphi_{h1})+b_2(\theta_1-\varphi_{h1}) \\ \frac{\partial\varphi_{h2}}{\partial\tau} = b_1(\theta-\varphi_{h2})+b_2(\theta_2-\varphi_{h2}) \\ \frac{\partial\varphi_s}{\partial\tau} = b_s(\theta-\varphi_s) \end{cases} \tag{13}$$

From the above equations, the 3rd order characteristic equation with complex coefficients can be obtained. The result is:

$$p^3 + p^2\left[rs + \frac{a_s's}{s+b_s} + \frac{2a'(s+b_2)}{s+b_1+b_2}\right] - p\left[s + \frac{a_1'(s+b_1)}{s+b_1+b_2}\right]^2 - s\left(s+\frac{a_1'(s+b_2)}{s+b_1+b_2}\right)\left[r\left(s+\frac{a_1'(s+b_1)}{s+b_1+b_2}\right)+2a'\frac{s+b_2+a_1'}{s+b_1+b_2}+\frac{a_s'}{s+b_s}\left(s+\frac{a_1'(s+b_1)}{s+b_1+b_2}\right)\right]=0 \tag{14}$$

and Equations (3) changes to

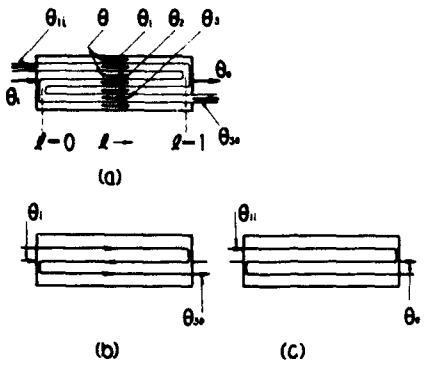

Fig.6 Case P-C, 1-3 pass heat exchanger.

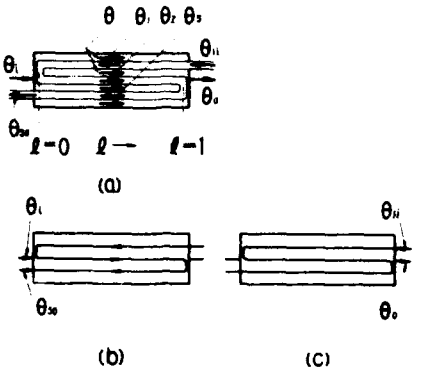

Fig.7 Case C-P, 1-3 pass heat exchanger.

$$\alpha=\frac{\frac{b_1}{s+b_1+b_2}a_1'}{-p+s+\frac{s+b_1}{s+b_1+b_2}a_1'},\quad \beta=\frac{\frac{b_1}{s+b_1+b_2}a_1'}{p+s+\frac{s+b_1}{s+b_1+b_2}a_1'} \tag{15}$$

The transfer functions may be obtained through a similar procedure.

1-3 Pass Heat Exchanger

Case P-C-P:

This is a parallel-counter-parallel flow heat exchange process. The fundamental equations are as follows, when no solid capacity exists.

$$\begin{cases} \frac{\partial\theta_1}{\partial\tau}+\frac{\partial\theta_1}{\partial l}=a_1(\theta-\theta_1) \\ \frac{\partial\theta_2}{\partial\tau}-\frac{\partial\theta_2}{\partial l}=a_1(\theta-\theta_2) \\ \frac{\partial\theta_3}{\partial\tau}+\frac{\partial\theta_3}{\partial l}=a_1(\theta-\theta_3) \\ r\frac{\partial\theta}{\partial\tau}+\frac{\partial\theta}{\partial l}=a(\theta_1-\theta)+a(\theta_2-\theta)+a(\theta_3-\theta) \end{cases} \tag{16}$$

The temperature variations of each fluid when input fluid temperature change is sinusoidal ($e^{s\tau}$) are:

$$\begin{cases} \theta_1=(\beta_1D_1e^{k_1l}+\beta_2D_2e^{k_2l}+\beta_3D_3e^{k_3l}+A_4e^{k_4l})e^{s\tau} \\ \theta_2=(\alpha_1D_1e^{k_1l}+\alpha_2D_2e^{k_2l}+\alpha_3D_3e^{k_3l})e^{s\tau} \\ \theta_3=(\beta_1D_1e^{k_1l}+\beta_2D_2e^{k_2l}+\beta_3D_3e^{k_3l}-A_4e^{k_4l})e^{s\tau} \\ \theta=(D_1e^{k_1l}+D_2e^{k_2l}+D_3e^{k_3l})e^{s\tau} \end{cases} \tag{17}$$

where, D_1, D_2, D_3, A_4 are the constants of integration, and p_1,p_2,p_3 are the roots of

$$p^3 + p^2(3a+rs) - p\{(a_1+s)^2 + 2aa_1\} - s(s+a_1)\{r(a_1+s)+3a\} = 0 \qquad (18)$$

and $p_4 = -(a_1 + s)$ (19)

The α, β are given by equation (3).

If shell input is considered, from the similar boundary conditions as 1-2 pass type, as shown in Fig.6(b), the constants of integration are determined and the transfer function $G_{PCP-st}(s) = \theta_{30}/\theta_i$ is obtained:

$$G_{pcp-st}(s) = [(\alpha_2\beta_1 - \alpha_1\beta_2)(2\beta_3 - \alpha_3)(e^{p_1+p_2} - e^{p_3+p_4}) + (\alpha_3\beta_2 - \alpha_2\beta_3)(2\beta_1 - \alpha_1)(e^{p_2+p_3} - e^{p_4+p_1}) + (\alpha_1\beta_3 - \alpha_3\beta_1)(2\beta_2 - \alpha_2)(e^{p_3+p_1} - e^{p_2+p_4})]/\Delta_3 \qquad (20)$$

where, $\Delta_3 = e^{p_1}(\alpha_1 - \beta_1)[2(\beta_2 - \beta_3) - (\alpha_2 - \alpha_3)] + e^{p_2}(\alpha_2 - \beta_2)[2(\beta_3 - \beta_1) - (\alpha_3 - \alpha_1)]$

$$+ e^{p_3}(\alpha_3 - \beta_3)[2(\beta_1 - \beta_2) - (\alpha_1 - \alpha_2)] + e^{p_4}[\alpha_1(\beta_2 - \beta_3) + \alpha_2(\beta_3 - \beta_1) + \alpha_3(\beta_1 - \beta_2)] \qquad (21)$$

Changing input and output relations as in Fig.6(c), we get

$$G_{pcp-ts}(s) = [\{(\alpha_1 - \beta_1) - (\alpha_2 - \beta_2)\}(e^{p_1+p_2} - e^{p_3+p_4}) + \{(\alpha_2 - \beta_2) - (\alpha_3 - \beta_3)\}(e^{p_2+p_3} - e^{p_1+p_4}) + \{(\alpha_3 - \beta_3) - (\alpha_1 - \beta_1)\}(e^{p_3+p_1} - e^{p_2+p_4})]/\Delta_3 \qquad (22)$$

Case C-P-C:

This is the case of counter-parallel-counter flow heat exchange process. See Fig.7(a). The fundamental equations are:

$$\begin{cases} \frac{\partial\theta_1}{\partial\tau} - \frac{\partial\theta_1}{\partial\ell} = a_1(\theta - \theta_1) \\ \frac{\partial\theta_2}{\partial\tau} + \frac{\partial\theta_2}{\partial\ell} = a_1(\theta - \theta_2) \\ \frac{\partial\theta_3}{\partial\tau} - \frac{\partial\theta_3}{\partial\ell} = a_1(\theta - \theta_3) \\ r\frac{\partial\theta}{\partial\tau} + \frac{\partial\theta}{\partial\ell} = a(\theta_1 - \theta) + a(\theta_2 - \theta) + a(\theta_3 - \theta) \end{cases} \qquad (23)$$

From which we get

$$\begin{cases} \theta_1 = (\alpha_1 D_1 e^{p_1\ell} + \alpha_2 D_2 e^{p_2\ell} + \alpha_3 D_3 e^{p_3\ell} + A_5 e^{p_5\ell})e^{s\tau} \\ \theta_2 = (\beta_1 D_1 e^{p_1\ell} + \beta_2 D_2 e^{p_2\ell} + \beta_3 D_3 e^{p_3\ell})e^{s\tau} \\ \theta_3 = (\alpha_1 D_1 e^{p_1\ell} + \alpha_2 D_2 e^{p_2\ell} + \alpha_3 D_3 e^{p_3\ell} - A_5 e^{p_5\ell})e^{s\tau} \\ \theta = (D_1 e^{p_1\ell} + D_2 e^{p_2\ell} + D_3 e^{p_3\ell})e^{s\tau} \end{cases} \qquad (24)$$

where, D_1, D_2, D_3, A_5 are the integration constants and p_1, p_2, p_3 are the three roots of

$$p^3 + p^2(3a + rs) - b\{(a_1+s)^2 - aa_1\} - s(s+a_1)\{r(a_1+s) + 3a\} = 0 \tag{25}$$

and $$p_5 = a_1 + s \tag{26}$$

α, β can be expressed by Equation (3) as before.

Shell side input: From the boundary conditions shown in Fig.7(b), we get the following transfer function through a similar procedure as before.

$$\begin{aligned} G_{cpc-st}(s) = [&(2\alpha_3 - \beta_3)(\alpha_1\beta_2 - \alpha_2\beta_1)(e^{p_1+p_2} - e^{p_3+p_5}) \\ &+ (2\alpha_1 - \beta_1)(\alpha_2\beta_3 - \alpha_3\beta_2)(e^{p_2+p_3} - e^{p_1+p_5}) \\ &+ (2\alpha_2 - \beta_2)(\alpha_3\beta_1 - \alpha_1\beta_3)(e^{p_3+p_1} - e^{p_2+p_5})]/\Delta_3' \end{aligned} \tag{27}$$

where, $$\Delta_3' = e^{p_1+p_2}(\alpha_1\beta_2 - \alpha_2\beta_1) + e^{p_2+p_3}(\alpha_2\beta_3 - \alpha_3\beta_2) + e^{p_3+p_1}(\alpha_3\beta_1 - \alpha_1\beta_3)$$
$$+ e^{p_5}[e^{p_1}(2\alpha_1 - \beta_1)(\alpha_3 - \beta_3 - \alpha_2 + \beta_2) + e^{p_2}(2\alpha_2 - \beta_2)(\alpha_1 - \beta_1 - \alpha_3 + \beta_3) + e^{p_3}(2\alpha_3 - \beta_3)(\alpha_2 - \beta_2 - \alpha_1 + \beta_1)] \tag{28}$$

Tube side input: From the boundary conditions in Fig.7(c), we get the following result:

$$\begin{aligned} G_{cpc-ts}(s) = [&\{(\alpha_1 - \beta_1) - (\alpha_2 - \beta_2)\}(e^{p_1+p_2} - e^{p_3+p_5}) + \{(\alpha_2 - \beta_2) - (\alpha_3 - \beta_3)\}(e^{p_2+p_3} - e^{p_1+p_5}) \\ &+ \{(\alpha_3 - \beta_3) - (\alpha_1 - \beta_1)\}(e^{p_3+p_1} - e^{p_2+p_5})]/\Delta_3' \end{aligned} \tag{29}$$

1-4 Pass Heat Exchanger

Case P-C-P-C: Assuming as before, the fundamental equations are:

$$\begin{cases} \dfrac{\partial\theta}{\partial\tau} + \dfrac{\partial\theta}{\partial\ell} = a_1(\theta - \theta_1) \\ \dfrac{\partial\theta_2}{\partial\tau} - \dfrac{\partial\theta_2}{\partial\ell} = a_1(\theta - \theta_2) \\ \dfrac{\partial\theta_3}{\partial\tau} + \dfrac{\partial\theta_3}{\partial\ell} = a_1(\theta - \theta_3) \\ \dfrac{\partial\theta_4}{\partial\tau} - \dfrac{\partial\theta_4}{\partial\ell} = a_1(\theta - \theta_4) \\ 4\dfrac{\partial\theta}{\partial\tau} + \dfrac{\partial\theta}{\partial\ell} = a(\theta_1 - \theta) + a(\theta_2 - \theta) + a(\theta_3 - \theta) + a(\theta_4 - \theta) \end{cases} \tag{30}$$

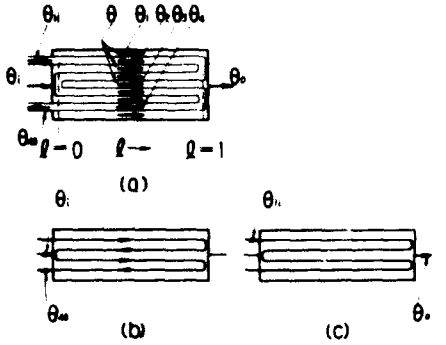

Fig.8 Case P-C-P-C, 1-4 pass heat exchanger.

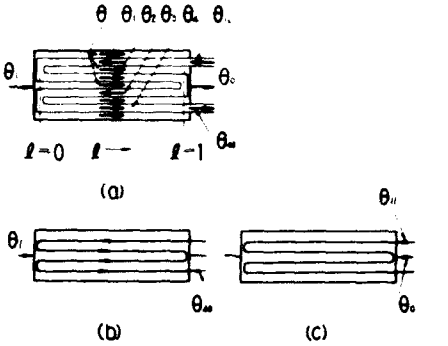

Fig.9 Case C-P-C-P, 1-4 pass heat exchanger.

From which, we get

$$\begin{cases} \theta_1 = (\beta_1 E_1 e^{p_1 l} + \beta_2 E_2 e^{p_2 l} + \beta_3 E_3 e^{p_3 l} + A_4 e^{p_4 l})\, e^{s\tau} \\ \theta_2 = (\alpha_1 E_1 e^{p_1 l} + \alpha_2 E_2 e^{p_2 l} + \alpha_3 E_3 e^{p_3 l} + B_5 e^{p_5 l})\, e^{s\tau} \\ \theta_3 = (\beta_1 E_1 e^{p_1 l} + \beta_2 E_2 e^{p_2 l} + \beta_3 E_3 e^{p_3 l} - A_4 e^{p_4 l})\, e^{s\tau} \\ \theta_4 = (\alpha_1 E_1 e^{p_1 l} + \alpha_2 E_2 e^{p_2 l} + \alpha_3 E_3 e^{p_3 l} - B_5 e^{p_5 l})\, e^{s\tau} \\ \theta = (E_1 e^{p_1 l} + E_2 e^{p_2 l} + E_3 e^{p_3 l})\, e^{s\tau} \end{cases} \tag{31}$$

where, E_1, E_2, E_3, A_4, B_5 are the constants of integration, α, β are obtained from Equation (3), and p_1, p_2, p_3 are the three roots of the following equation.

$$p^3 + p^2(4a + rs) - p(a_1 + s)^2 - s(s + a_1)\{r(a_1 + s) + 4a\} = 0 \tag{32}$$

$$p_4 = -(a_1 + s) \tag{33}$$

$$p_5 = a_1 + s \tag{34}$$

Shell input: From the boundary conditions shown in Fig.8(b), we get the transfer function

$$G_{pcpc\text{-}st}(s) = 2(e^{p_4} + e^{p_5})[(\alpha_1 - \beta_1)(\alpha_2\beta_3 - \alpha_3\beta_2)e^{p_1} + (\alpha_2 - \beta_2)(\alpha_3\beta_1 - \alpha_1\beta_3)e^{p_2} + (\alpha_3 - \beta_3)(\alpha_1\beta_2 - \alpha_2\beta_1)e^{p_3}]/\Delta_4 \tag{35}$$

where, $\Delta_4 = e^{p_5}[(\alpha_1 - \beta_1)\{\alpha_2 - \alpha_3 - 2(\beta_2 - \beta_3)\}e^{p_1} + (\alpha_2 - \beta_2)\{\alpha_3 - \alpha_1 - 2(\beta_3 - \beta_1)\}e^{p_2} + (\alpha_3 - \beta_3)\{\alpha_1 - \alpha_2 - 2(\beta_1 - \beta_2)\}e^{p_3} + e^{p_4}[(\alpha_1 - \beta_1)(\beta_3 - \beta_2)e^{p_1} + (\alpha_2 - \beta_2)(\beta_1 - \beta_3)e^{p_2} + (\alpha_3 - \beta_3)(\beta_2 - \beta_1)e^{p_3}]$

Tube input: See Fig.8(c). The transfer function is:

$$G_{pcpc-ts}(s) = (e^{p_4} + e^{p_5})\left[\{(\alpha_2-\beta_2)-(\alpha_1-\beta_1)\}e^{p_1+p_2} + \{(\alpha_3-\beta_3)-(\alpha_2-\beta_2)\}e^{p_2+p_3} + \{(\alpha_1-\beta_1)-(\alpha_3-\beta_3)\}e^{p_3+p_1}\right]/\Delta_4 \quad (36)$$

Case C-P-C-P: The fundamental equations are,

$$\begin{cases} \frac{\partial\theta}{\partial\tau} - \frac{\partial\theta_1}{\partial\ell} = a_1(\theta-\theta_1) \\ \frac{\partial\theta_2}{\partial\tau} + \frac{\partial\theta_2}{\partial\ell} = a_1(\theta-\theta_2) \\ \frac{\partial\theta_3}{\partial\tau} - \frac{\partial\theta_3}{\partial\ell} = a_1(\theta-\theta_3) \\ \frac{\partial\theta_4}{\partial\tau} + \frac{\partial\theta_4}{\partial\ell} = a_1(\theta-\theta_4) \\ r\frac{\partial\theta}{\partial\tau} + \frac{\partial\theta}{\partial\ell} = a(\theta_1-\theta)+a(\theta_2-\theta)+a(\theta_3-\theta)+a(\theta_4-\theta) \end{cases} \quad (37)$$

The transfer functions can be obtained through the procedure described before:

Shell input: See Fig.9(b).

$$G_{cpcp-st}(s) = 2(e^{p_4} + e^{p_5})\left[(\alpha_3-\beta_3)(\alpha_1\beta_2-\alpha_2\beta_1)e^{p_1+p_2} + (\alpha_1-\beta_1)(\alpha_2\beta_3-\alpha_3\beta_2)e^{p_2+p_3} + (\alpha_2-\beta_2)(\alpha_3\beta_1-\alpha_1\beta_3)e^{p_3+p_1}\right]/\Delta_4' \quad (38)$$

Tube input: See Fig.9(c).

$$G_{cpcp-ts}(s) = (e^{p_4} + e^{p_5})\left[\{(\alpha_3-\beta_3)-(\alpha_2-\beta_2)\}e^{p_1} + \{(\alpha_1-\beta_1)-(\alpha_3-\beta_3)\}e^{p_2} + \{(\alpha_2-\beta_2)-(\alpha_1-\beta_1)\}e^{p_3}\right]/\Delta_4' \quad (39)$$

where, p_1, p_2, p_3 are the roots of Equation (32), α, β are to be obtained from Equations (3), and p_4, p_5 are given by Equations (33) and (34) respectively.

and,
$$\Delta_4' = e^{p_5}\left[\{(\alpha_3-\beta_3)-(\alpha_2-\beta_2)\}(2\alpha_1-\beta_1)e^{p_1} + \{(\alpha_1-\beta_1)-(\alpha_3-\beta_3)\}(2\alpha_2-\beta_2)e^{p_2} + \{(\alpha_2-\beta_2)-(\alpha_1-\beta_1)\}(2\alpha_3-\beta_3)e^{p_3}\right] + e^{p_4}\left[\alpha_1\{(\alpha_3-\beta_3)-(\alpha_2-\beta_2)\}e^{p_1} + \alpha_2\{(\alpha_1-\beta_1)-(\alpha_3-\beta_3)\}e^{p_2} + \alpha_3\{(\alpha_2-\beta_2)-(\alpha_1-\beta_1)\}e^{p_3}\right] \quad (40)$$

Cases With More Than Four Tube-passes

The above mentioned procedures can be equally applied to the heat exchangers which have more than four tube-passes.

The procedure is rather complicated when the number of tube-pass is odd.

For example, let us consider the (2n+1) pass heat exchanger:

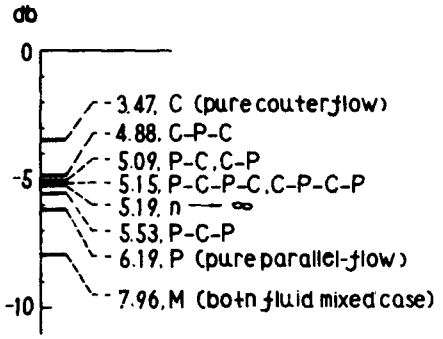

Fig.10 Comparison of static characteristics of multipass heat exchangers for r = 1, total a_1 = total a = 2.

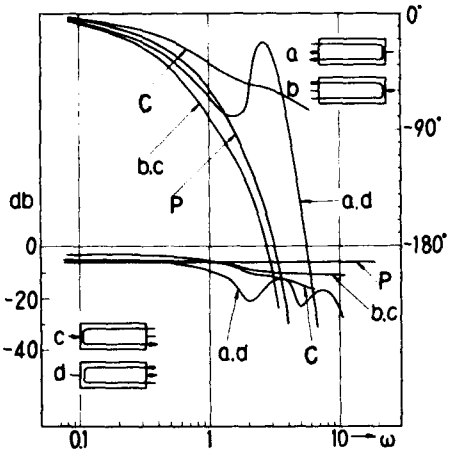

Fig.11 Frequency response of 1-2 pass heat exchangers for r = 1, a_1 = 1.

The 3rd order characteristic equation is;

For the types P-C-P------

$$p^3+p^2\{(2n+1)a+rs\}-p\{(a_1+s)^2+aa_1\}-s(s+a_1)\{r(a_1+s)+(2n+1)a\}=0 \qquad (41)$$

which corresponds to Equation (18). The remainder p values are given by n, n-1 repeated roots of p_4, p_5 respectively.

For the types C-P-C------

$$p^3+p^2\{(2n+1)a+rs\}-p\{(a_1+s)^2-aa_1\}-s(s+a_1)\{r(a_1+s)+(2n+1)a\}=0 \qquad (42)$$

which corresponds to Equation (25). The remainder p values are given by n-1, n repeated roots of p_4, p_5 respectively.

For the (2n) pass heat exchanger, the characteristic equation corresponding to Equations (4) and (32) is as follows for both P-C-P-C------ and C-P-C-P------ :

$$p^3+p^2(2na+rs)-p(a_1+s)^2-s(s+a_1)\{r(s+a_1)+2na\}=0 \qquad (43)$$

The remainder p values are given by n-1 repeated roots of p_4, p_5.

Thus, the dynamic response of these multi-pass heat exchangers can be obtained through the use of these roots. The order of the equations never exceeds three so long as all tube-passes are identical and the number of shell pass is one.

If the number of tube-pass approaches infinity, this method becomes very complicated, but on the other hand the temperature gradient in

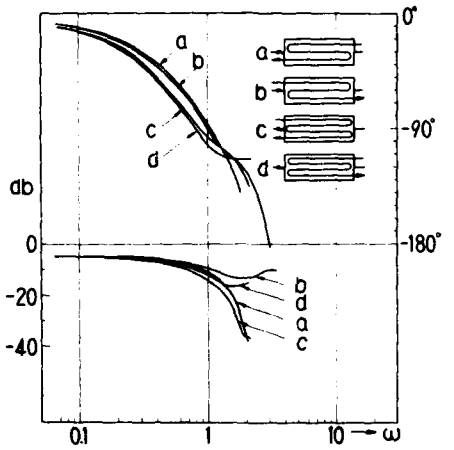

Fig.12 Frequency response of 1-3, 1-4 pass heat exchangers for shell-side input, r = 1, total a_1 = total a = 2.

one tubepass becomes almost zero, therefore we can consider this case as a crossflow type heat exchanger with both fluids mixed normal to the directions of flow respectively. The static characteristics of this case has already been obtained [15]. Although the dynamic response of it is relatively easy to obtain, since the dead time may not essentially be equal, the phase characteristics can not be obtained. Consequently, we can use only the static response formulas to obtain the limiting value of dc gain in this case.

Numerical Example of Frequency Response

Static and dynamic responses are compared using the obtained transfer function formulas neglecting the heat capacities of solid. A set of the system parameters used are: r = 1, total a_1 = total a = 2. In other words, equal heat exchange conditions for all heat exchangers are assumed.

Fig.10 shows that the dc gain patterns possess quite systematic relations each other. Note that the response of a heat exchanger with more than two tube-passes lies between C and P. Also note that as the number of tube-passes increases, the effects of counter-and parallel-flow in individual passes are averaged each other and the response approaches to the value when the number of tube-pass is infinity.

Fig.11 shows the frequency response of 1-2 pass heat exchanger. Note that the phase curves of $G_{PC-st}(j\omega)$ and $G_{CP-ts}(j\omega)$ has a

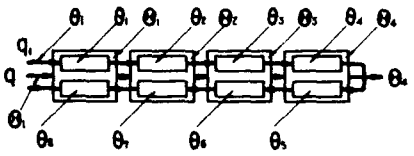

(a) Lumped-parameter model of 1-2 pass heat exchanger.

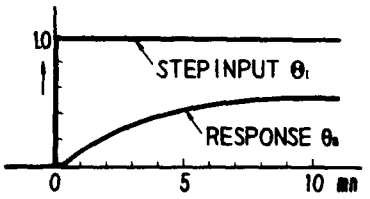

(c)-1 Indicial response.

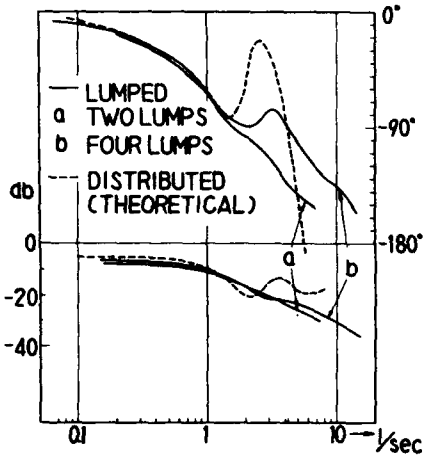

(c)-2 Frequency response for shell-input.

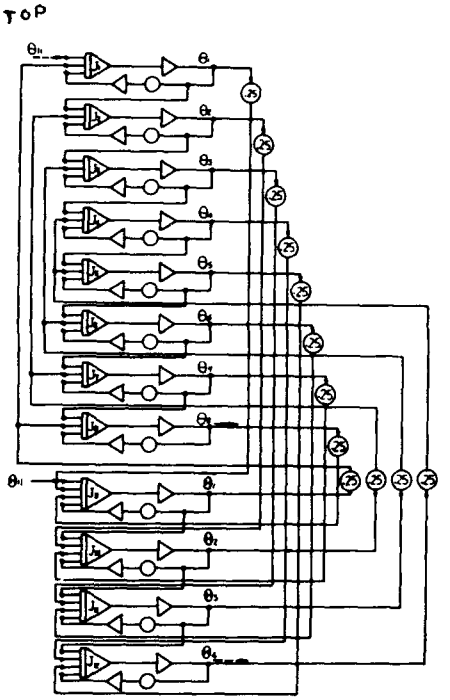

(b) Analog computer circuit.

Fig.13 Analog-computer test.

peak value and gain curves are oscillatory for a certain frequency range. P and C denote the responses of the pure parallel and counter-flow heat exchangers respectively.

Fig.12 shows the responses of the 1-3, 1-4 pass heat exchangers for shell input. Note that the response curves may be oscillatory about $\omega > 1.5$.

From Figs.11, 12, following results may be observed and summarized:

(1) The phase lag increases with the number of tube-passes.

(2) In the very low frequency range, the gain approaches to the value given by the dc gain and phase lag is small, which means the whole length of shell-pass and tube-pass are effective.

(3) In the medium frequency range, input and output relations have a marked effect on the frequency response characteristics.

(4) In the high frequency range, both the phase and the gain curves become oscillatory for $\omega > 1.5$, which might be due to the interaction between shell-pass and tube-pass.

(5) The phase lag would be larger and the gain would be more attenuated when solid capacities are added in a practical heat exchanger, especially at high frequency range.

Analog Computer Test

Although several analog circuits for a pure parallel-and counter-flow heat exchanger have already been published [16],[17], the author devised a simpler method using ordinary analog computer to investigate the dynamic response.

Considering case P-C and dividing the heat exchanger with no wall capacity as shown in Fig.13(a) to four equal lumped systems, gives

$$
\begin{cases}
\frac{d\theta_1}{d\tau} + (a_1+1)\theta_1 = \theta_{1i} + a_1\Theta_1 \\
\frac{d\theta_2}{d\tau} + (a_1+1)\theta_2 = \theta_1 + a_1\Theta_2 \\
\frac{d\theta_3}{d\tau} + (a_1+1)\theta_3 = \theta_2 + a_1\Theta_3 \\
\frac{d\theta_4}{d\tau} + (a_1+1)\theta_4 = \theta_3 + a_1\Theta_4 \\
\frac{d\theta_5}{d\tau} + (a_1+1)\theta_5 = \theta_4 + a_1\Theta_4 \\
\frac{d\theta_6}{d\tau} + (a_1+1)\theta_6 = \theta_5 + a_1\Theta_3 \\
\frac{d\theta_7}{d\tau} + (a_1+1)\theta_7 = \theta_6 + a_1\Theta_2 \\
\frac{d\theta_8}{d\tau} + (a_1+1)\theta_8 = \theta_7 + a_1\Theta_1 \\
r\frac{d\Theta_1}{d\tau} + (2a+1)\Theta_1 = \Theta_i + a(\theta_1+\theta_8) \\
r\frac{d\Theta_2}{d\tau} + (2a+1)\Theta_2 = \Theta_1 + a(\theta_2+\theta_7) \\
r\frac{d\Theta_3}{d\tau} + (2a+1)\Theta_3 = \Theta_2 + a(\theta_3+\theta_6) \\
r\frac{d\Theta_4}{d\tau} + (2a+1)\Theta_4 = \Theta_3 + a(\theta_4+\theta_5)
\end{cases}
\tag{44}
$$

The analog computer circuit using the same system parameters as in the former numerical example is shown in Fig.13(b).

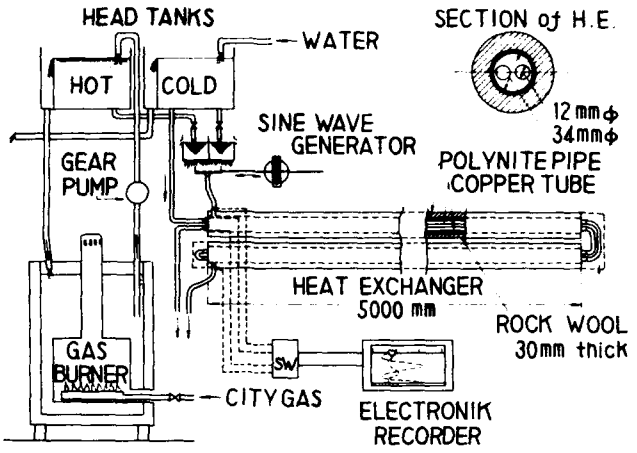

Fig.14 Schematic diagram of experimental apparatus, frequency-response measurement.

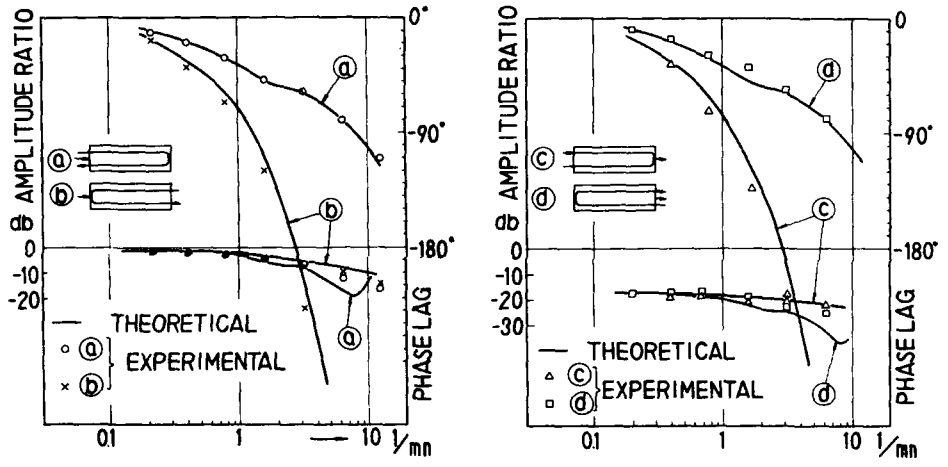

(a) Frequency responses for shell-side input.

(b) Frequency responses for tube-side input.

Fig.15 Experimental results.

Fig.13(c) shows the frequency response and the transient response for shell-side input. In some frequency ranges the phase curve shows evidently a peak value, which would approach the one for the exact distributed system as the number of lumps increases.

Experimental Results

The frequency response of the multi-pass heat exchanger is quite different than the others for 1-2 pass as has been demonstrated by the numerical example of Fig.11 and Fig.12.

The author has made experiments on a two-pass heat exchanger as shown in Fig.14. The length of the heat exchanger was chosen 10 meters

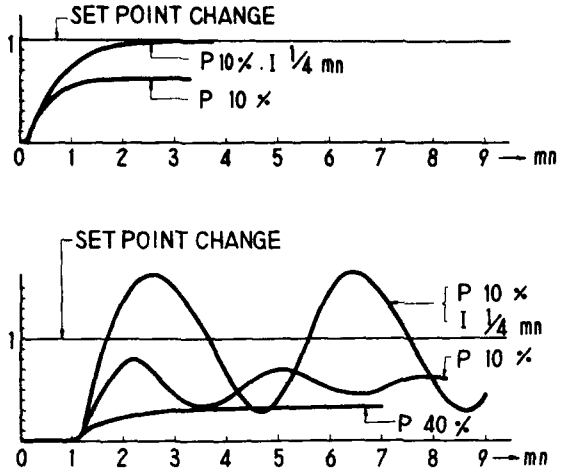

Fig.17 Closed-loop transient responses to step-function disturbances, upper diagram shows the responses for (a) in Fig.15(a), lower diagram shows the responses for (b) in Fig.15(a).

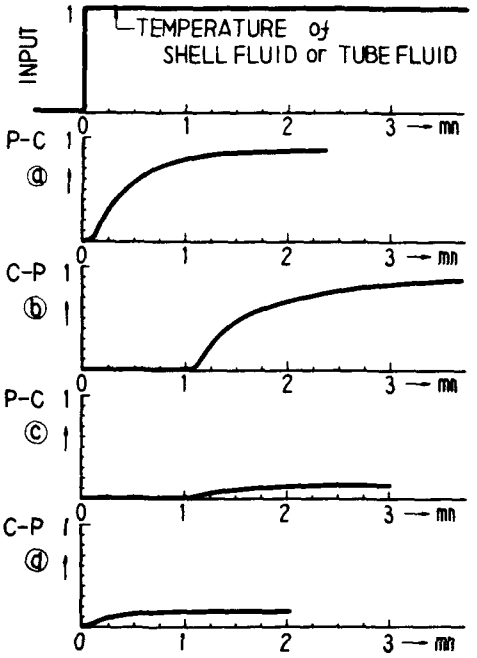

Fig.16 Indicial responses.

so as to cover theoretical peak of the phase shift curve. The heat exchange process is water-to-water. The shell material was "polynite" in order to decrease the effects of side capacity: tube-pass was thin (0.3 mm) copper tube. The test conditions are:

$A = 0.368\ m^2$
$C_h = 8.815 \times 10^{-3}$ kcal/m°C
$C_s = 122.7 \times 10^{-3}$ kcal/m°C
$H = 10$ m
$L_1 = H/v_1 = 1$ mn
$v_1 = v \div 10$ m/mn, $r = 1$
$w_1 = 0.102$ kcal/m°C
$w = 0.682$ kcal/m°C

	for shell-side input	for tube-side input
a_1	3.01	2.86
a	0.45	0.43
a_1'	5.94	6.12
a'	0.92	0.81
a_s'	0.046	0.04
b_1	70.8	62.5
b_2	68.7	70.8
b_s	0.25	0.22

Temperature was recorded by Yamatake-Honeywell Electronik Potentiometer with bare Cu-constantan wire (0.2 mm ϕ) as the temperature

sensing elements, the response speed of which is sufficiently high for the dynamic response measurements.

The experimental results which involve the effects of series and side capacities are shown in Figs.15, 16.

Fig.15(a) shows the frequency responses for shell-side input, (b) for tube-side input. Favorable agreements are seen between the theoretical and the experimental results. Four cases in Fig.15 each corresponds to the four cases in Fig.16 which shows the transient responses.

Note that the phase shift characteristics of case ⓐ is quite similar to that of case ⓓ , but the gain characteristics is different, this may be due to the difference between the heat capacities of the input side fluid and output side fluid.

Although the same remarks can be said for the cases ⓒ, ⓑ, the effects of large dead time are remarkable.

Control of 1-2 Pass Heat Exchanger

As can be seen from the experimental results, the choice of input and output are especially important for control applications. This fact can be evidently seen in the closed loop response as follows:

Fig.17 shows the responses for shell-side input when P and PI control actions were used.

Above figure in Fig.17 resulting from the case ⓐ in Fig.15 shows very stable response; lower one from the case ⓑ in Fig.15 shows far unstable response.

Acknowlegements

The author particularly wishes to acknowlege the earnest encouragement and guide for the research received from Prof. Y.Takahashi, University of California, and also to acknowlege the useful suggestions from Prof. T.Node, Yokohama National University.

The author is also grateful to Mr. S.Aoki, the head of the Tsurumi Laboratory, and Mr. E.Suzuki at the Tsurumi Laboratory, Tokyo Shibaura Electric Company, for their permission and help to use the low-speed analog computer TOSAC-II; to Mr. G.Kako and S.Ogawa at Yamatake-Honeywell Instrument Company for their cordial permission to use the Electronik Recorder and Controller.

Finally, the author is grateful to Mr. T.Noguchi, H.Kurashima and K.Yamanouchi, students at Yokohama National University, who assisted in the numerical calculations and experimental measurements.

BIBLIOGRAPHY

(1) "Transfer Function Analysis of Heat Exchange Processes," by Y.Takahashi, edited by A.Tustin, Automatic and Manual Control, Butterworths, London, 1952, p.235

(2) "Regeltechnische Eigenschaften von Gleich-und Gegenstromwärme-austauschern," by Y.Takahashi, Regelungstechnik, Heft 2, 1953, s.32-35

(3) " A New Method of Evaluating Dynamic Response of Counterflow and Parallel-Flow Heat Exchangers," by H.M.Paynter and Y.Takahashi, Trans. ASME, vol.78, no.4, 1956, pp.749-758

(4) "Dynamic Characteristics of Double-Pipe Heat Exchangers," by W.C.Cohen and E.F.Johnson, Industrial and Engineering Chemistry, vol.48, June, 1956, pp.1031-1034

(5) "Dynamic Analysis of Heat Exchanger Control," by B.D.Hainsworth, V.V.Tivy and H.M.Paynter, ISA Journal, vol.4, no.6, June, 1957, p.230

(6) "Mean Temperature Difference in Multipass Heat Exchangers," by W.M.Nagle, Industrial and Engineering Chemistry, vol.25, 1933, pp.604-609

(7) "The Calculation of the Mean Temperature Difference in Multipass Heat Exchangers," by A.J.V.Underwood, Journal of the Institution of Petroleum Technologists, vol.20, 1934, pp.145-158

(8) "Mean Temperature Difference Correction in Multipass Exchangers," by R.A.Bowman, Industrial and Engineering Chemistry, vol.28, May, 1936, pp.541-544

(9) "Mean Temperature Difference Correction in Multipass Exchangers," by F.K.Fischer, Industrial and Engineering Chemistry, vol.30, April, 1938, pp.377-383

(10) "Mean Temperature Difference in Design," by R.A.Bowman, A.C.Mueller and W.M.Nagle, Trans. ASME, vol.62, 1940, pp.283-294

(11) " Multi-Pass Heat Exchangers," by T.Node, Transactions of the Japan Society of Mechanical Engineers, vol.6, no.22, 1940, pp.II 19-37

(12) "Die Behandlung von Regelproblemen vermittels des Frequenzganges des Regelkreises," by P.Profos, Diss. Zürich, 1943

(13) "Control of Multi-Pass Heat Exchangers(Part 1, Dynamic Character-

istics of Two-Pass Heat Exchanger)," by M.Masubuchi, Transactions of the Japan Society of Mechanical Engineers, vol.24, no.139, March, 1958, pp.209-213

(14) "Einheitliche Berechnung von Rekuperatoren," by V.Bošnjaković, M.Vilič́ić and B.Slipčević, VDI-Forschungsheft 432, 17, 1951, z.5-26

(15) "Mean Temperature Difference in Cross Flow," by D.M.Smith, Engineering, vol.138, 1934, pp.479-481, 606-607

(16) "Electrical Analogues for Heat Exchangers," by R.L.Ford, Proc. IEE Paper, no.1934, vol.103, no.7, Jan., 1956, pp.65-82

(17) "Die elektrische Nachbildung der instationären thermischen Vorgänge beim Wärmeaustauschern," by G.Kourim, Regelungstechnik, Heft 5, 1957, z.163-167

Appendix

A technique for obtaining the roots of the characteristic equation is to be described. In general, the third-order characteristic equations with $s = j\omega$ may be written in the form

$$p^3 + p^2 (m_1 + jn_1) + p (m_2 + jn_2) + m_3 + jn_3 = 0 \qquad (45)$$

where m's and n's are real numbers, and are function of the variable ω.

Substituting $p = u + jv$ into the above equation, and equating both the real and the imaginary parts to zero yield the following two equations.

$$\begin{aligned} &u^3 + u^2 m_1 + u(m_2 - 2vn_1 - 3v^2) - v^2 m_1 - vn_2 + m_3 = 0 \\ &v^3 + v^2 n_1 + v(- m_2 - 2um_1 - 3u^2) - u^2 n_1 - un_2 - n_3 = 0 \end{aligned} \qquad (46)$$

Three pairs of curves can be drawn on the u-v complex plane from these two equations, and the three roots p_1, p_2 and p_3 can be found from the intersecting points of the curves.

As an example, consider Equation (4) with $r = 1$, and $a_1 = a = 1$. By letting $s = j\omega$, the equation becomes

$$p^3 + p^2(2 + j\omega) + p(\omega^2 - 1 - 2j\omega) + 4\omega^2 + j\omega (\omega^2 - 3) = 0 \qquad (47)$$

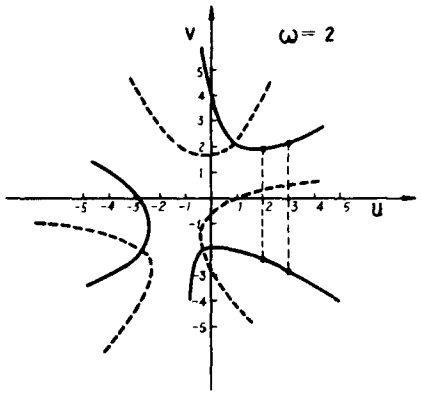

Fig.18 Auxiliary curves to obtain the roots of Equation (47).

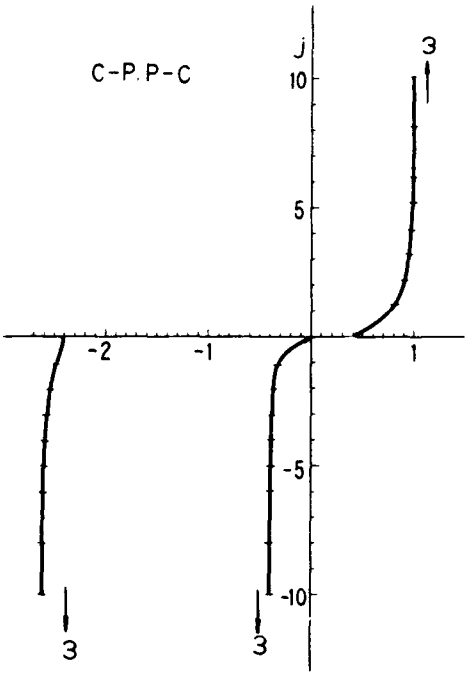

Fig.19 Three roots of characteristic equation on complex plane for r = 1, $a_1 = a = 1$.

In order to find the values of p's for $\omega = 2$, first, the pair of equations corresponding to Equation (46) are found.

$$u^3 + 2u^2 + u(-3v^2 - 4v + 3) - 2v^2 + 4v + 16 = 0 \qquad (48)$$

$$v^3 + 2v^2 + v(-3u^2 - 4u - 3) - 2u^2 + 4u - 2 = 0 \qquad (49)$$

By letting u = 3,2,1,0, and etc. in Equation (48), two values of v's that satisfy the equation are evaluated for each value of u. The result is the u-curves shown in solid lines in Fig.18. The v-curves are obtained in likewise manner, and are shown in dotted lines in the same figure. The three intersecting points are the roots of the Equation (47).

Although the accuracy of the p's may be improved by expanding the u, v scale about the points of intersection, the following technique used by the author is recommended for its simplicity.

Considering the regeon $u > 0$, $v > 0$ only, and expanding scales, one obtain $p_1 = 0.89 + j\,2.16$. Next, divide Equation (47) with $\omega = 2$ by p- 0.89- j 2.16.

$$p^2 + p(2.89+j4.16) \quad -3.4135+j5.9448 \qquad \text{———————(a)}$$

$$p-0.89-j2.16 \;\big)\; p^3 + p^2(2 \quad +j2 \quad) + p(3 \quad -j4 \quad) + 16 \quad +j2$$

$$p^3 - p^2(0.89+j2.16)$$

$$p^2(2.89+j4.16) + p(3 \quad -j4 \quad)$$

$$p^2(2.89+j4.16) + p(6.4135-j9.9448)$$

$$p(-3.4135+j5.9448)$$

$$p(-3.4135+j5.9448) + 15.878783 + j2.082288$$

$$0.121217 - j0.082288$$

$$\text{————(b)}$$

In this division, 0.89 and 2.16 are modified individually so as to reduce the residual (b) as small as possible. The final results are 0.8950 and 2.1630. Then from the quotient (a), obtained through this procedure, the rest of p values can be easily obtained. The values are:

$$p_2 = -2.5320 - j\,2.0902$$

$$p_3 = -0.3629 - j\,2.0728$$

Although this division may appear to be rather troublesome, this is more efficient than obtaining each intersecting points separately.

Applying the same procedure for each ω, other p values can be obtained as shown in Fig.19